Scalable Machine Learning Models for Predicting Quantum Transport in Disordered 2D Hexagonal Materials

Seyed Mahdi Mastoor[1] and Amirhossein Ahmadkhan Kordbacheh[*2]

[1,2]Department of Physics, Iran University of Science and Technology, Tehran,Iran

We introduce scalable machine learning models to accurately predict two key quantum transport properties—the transmission coefficient T(E) and the local density of states (LDOS)—in two-dimensional (2D) hexagonal materials with magnetic disorder. Using a tight-binding Hamiltonian combined with the Non-Equilibrium Green's Function (NEGF) formalism, we generate a large dataset of over 400,000 unique configurations across graphene, germanene, silicene, and stanene nanoribbons with varying geometries, impurity concentrations, and energy levels. A central contribution of this work is the development of a geometry-driven, physically interpretable feature space that enables the models to generalize across material types and device sizes. Random Forest regression and classification models are evaluated in terms of accuracy, stability, and extrapolation ability. Regression consistently outperforms classification in capturing continuous transport behavior on in-domain data. However, extrapolation performance degrades significantly, revealing the limitations of tree-based models in unseen regimes. This study highlights both the potential and constraints of scalable ML models for quantum transport prediction and motivates future research into physics-informed or graph-based learning architectures for improved generalization in spintronic and nanoelectronic device design.

[*]akordbacheh@iust.ac.ir

1   Introduction

In recent years, research on two-dimensional (2D) materials has grown significantly due to their unique physical and electronic properties. These materials offer promising opportunities for the design and development of next-generation electronic and spintronic devices [1]. A wide variety of 2D materials can be created by stacking different monolayers to form heterostructures. Theoretical predictions suggest that nearly 5800 such materials exist, with around 1800 successfully synthesized in laboratories [2] [3]. Most 2D materials naturally adopt a hexagonal lattice structure, favored for its high stability and dense atomic packing [4].The atomic-scale thickness and remarkable transport properties of materials like graphene and germanene have made them central to advancements in nanoelectronics and spintronics[5][6].

There are different types of methods for investigating transport properties of materials. Among them, density functional theory (DFT) has been used widely for investigate electronic and spin properties. DFT cannot directly calculate transport properties; one of the methods for this aim is using the scattering matrix approach (S-matrix)[7].But S-matrix has constraint about non-equilibrium conditions. Non-equilibrium Green functions (NEGF) is an other method that can be used to study charge and spin transport. NEGF can handle out of equilibrium condition and also inelastic scattering[8][9]. However, substantial computational resources are often required when these traditional methods are applied to large or disordered systems, as they become computationally expensive.

To address these limitations, recent research has introduced novel machine learning (ML) and deep learning (DL) techniques to predict transport properties more efficiently. ML is becoming a powerful tool in the study of electron transport properties in nanoscale structures and materials with imputity and defects. One of its notable applications is the prediction of conductivity and transport probabilities in low-dimensional systems without the need to solve complex quantum transport equations [10] [11] [12][13]. Developing a reliable and scalable model to predict physical quantities such as transmission coefficients can be highly beneficial for researchers studying nanostructures and designing devices based on charge and spin transport [14].

The random forest algorithm is reported as a suitable model to predict transmission coefficients in the case that a regression problem converted to classification [15]. Since various 2D materials appear in hexagonal lattice shape [4]; In this work, models are presented to predict the transmission and local density of states (LDOS) of the hexagonal lattice. Models are made scalable by selecting a feature space related to lattice geometry, which has not been considered before. Besides, we compare the efficiency of regression versus classification methods to predict transmission and present the advantage and trade-off of each approach. The comparison seeks to guide researchers on choosing the right machine learning techniques for future quantum transport studies in low-dimensional systems.

2　Methodology

2.1　Tight binding model and non-equilibrium Green's function approach

We consider two-terminal device configurations, where the central scattering region contains magnetic impurities and is connected to non-magnetic leads on each sides (fig.1). The system is modeled using a tight-binding Hamiltonian of the form:

$$H = \sum_i \varepsilon_{i\sigma} C_{i\sigma} C_{i\sigma}^\dagger + \sum_{<ij>\sigma\sigma'} t_{ij}^{\sigma\sigma'} C_{j\sigma'} C_{i\sigma}^\dagger \tag{1}$$

where ε is the on-site energy and equal to $m_i \Delta \sigma_z$, where $m_i \in [-1, +1]$ denotes the randomly assigned local magnetic direction at site i, Also Δ as exchange energy set to unit. $t_{ij}^{\sigma\sigma'}$ present the hopping amplitude between sites i and j.

Graphene, germanene, silicene, and stanene—four of the most prominent 2D hexagonal lattice materials—are used to construct the dataset. These materials are chosen for their well-documented electronic properties, structural similarity, and relevance to emerging nanostructured device applications [16][17][18]. Including a diverse set of materials ensures that the trained models can generalize across a broader class of 2D hexagonal systems. For each material, numerous device configurations are calculated under varying physical conditions, such as geometry size and impurity concentration. This allows us to construct a comprehensive dataset of local density of states (LDOS) and transmission coefficients, in a position to capture the highly complex transport behavior inherent in hexagonal lattice structures. The hopping parameter are set based on material-specific values: -2.6 for graphene, -1.3 for germanene, -1.6 for silicene, and -0.79 for stanene. [19][20][21][22][23].

In order to establish that our models can generalize across many realistic device configurations, we vary the geometry of the scattering region by varying the number of atoms per unit cell from 6 to 32, and the number of unit cells in the transport direction from 1 to 7. The ranges we use yield narrow and wide nanoribbons as well as short and long devices within the realistic size ranges used as designs in nanoelectronics. We also randomly distributed magnetic impurities within the scattering region at a concentration of 0% to 10% of the total number of atomic sites. These ranges of concentration range from pristine systems to those with moderate disorder which allows the models to learn how the impurity-induced scattering affects transport processes. Altogether, the selections we have made provide a physically meaningful dataset that covers a large range, and enables the models to learn from an adequate set of training data that will be useful for scalable machine learning.

For each configuration, we compute two physical quantities that characterize the transport behavior: the transmission coefficient T(E) and LDOS, both calculated using the NEGF formalism. T(E) is calculated as:

$$T(E) = Trace[\Gamma_1 G^R \Gamma_2 G^A] \tag{2}$$
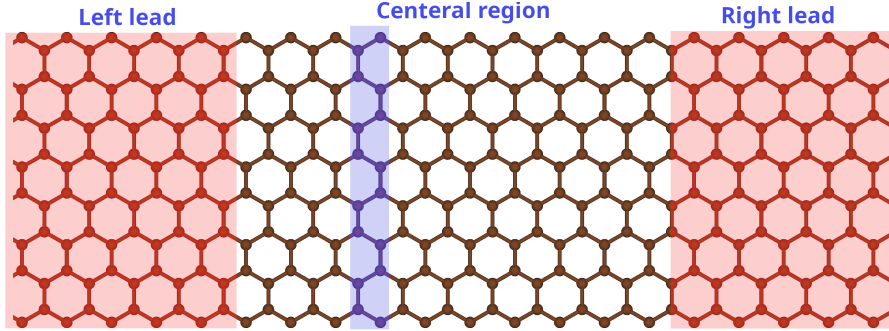
and LDOS :

Figure 1: Schematic of the two terminal device. Red color region represent leads and The unit cell is highlighted in blue.

$$LDOS_i = \frac{1}{2\pi} Im[G_i(E)] \tag{3}$$

where $G^{R,A} = [E - H - \Sigma_1^{R,A} - \Sigma_2^{R,A}]^{-1}$ is the retarded/advanced Green's function of the scattering region and $\Sigma_{1,2}^{R,A}$ being the retarded/advanced self energy of the left/ right electrode. Also Γ define as $\Gamma_{1,2} = i[\Sigma_{1,2}^R - \Sigma_{1,2}^A]$.

2.2 Machine learning

Physically meaningful parameters that specify the geometry and transport properties of the system are used to build the feature space. These collectively define the size and shape of the system and include the scattering region's width (number of atoms per unit cell, W), length (number of unit cells, L), total number of atoms (N) and the number of magnetic impurities (nm). We also take into account the target energy level at which the transmission T(E) and LDOS are calculated, and the hopping parameter, which varies depending on the material. This feature set enables the models to be general and scalable across various materials and configurations while capturing the fundamental physics governing quantum transport.

Random Forest (RF) classification and regression algorithms are employed in this research. RF is an ensemble learning method where numerous decision trees are generated during training and outputs are obtained from them, and it is extremely powerful and reliable for most prediction tasks [24] . Among the biggest strengths of Random Forest is that it has the ability to learn high-order nonlinear dependencies between features and target variables[25].

RF models are extremely scalable and effective when dealing with large datasets. Their parallelizability and the fact that they are inherently resilient to overfitting also mean that they are very effective at dealing with high-dimensional input spaces as well as noisy data [26]. In the application of quantum transport data, for instance, this characteristic makes RF highly suitable

where fine features are governed by very many interactive parameters such as geometry, disorder, and energy levels. Apart from Random Forest (RF), we also used Multilayer Perceptron (MLP) and Support Vector (SV) models to check their learning capacity of the complex, nonlinear relationships behind quantum transport data. MLP was chosen due to its capacity to map complex non-linear functions onto layered neural structure [27], and SV was included as a kernel-based model that is well known for its proficiency in handling high-dimensional and continuous feature spaces[28]. Both models have been successfully applied in physical and materials modeling experiments[29][30][31]. In our instance, although MLP and SVR yielded satisfactory results, Random Forest was better consistently in predictive accuracy, overfitting resistance, and computational efficiency. We thus selected RF as the base model for further evaluation, visualization, and interpretation in this study.

Performance of our machine learning models is assessed using popularly employed evaluation metrics. For regression tasks, we employ Mean Absolute Error (MAE), Root Mean Square Error (RMSE), and the coefficient of determination (R^2). These metrics help quantify how closely the predicted values match the actual continuous outputs, with lower MAE and RMSE indicating better performance, and R^2 indicating how well the model explains the variance in the data.

For classification tasks, we evaluate model performance using Accuracy and the F1-score. Accuracy measures the proportion of correctly predicted labels, while the F1-score—being the harmonic mean of precision and recall—provides a balanced view of the model's ability to classify each class correctly, especially useful when class distributions are imbalanced.

In order to avoid overfitting and have our models be good generalizers, we use k-fold cross-validation, dividing the dataset into training and validation sets multiple times. This provides a more reliable estimate of model performance. Additionally, we also use GridSearch to systematically explore different combinations of hyperparameters (such as the number of estimators, tree depth, and minimum samples per split) and then selecting the optimal configuration.

Furthermore, polynomial feature expansion is incorporated to capture nonlinear relationships between input features and target variables [32]. By transforming the original feature space onto interaction terms and higher-order components, we enable the models—particularly Random Forest—to learn the complex dependencies in our dataset better, which is essential given the nonlinearity of quantum transport phenomena in disordered systems.

3   Results

Dataset has been created by calculating $T(E)$ and LDOS for various shapes of scatter regions, as mentioned by the NEGF method. The energy range chosen for each material is by considering the transport energy window on the basis of the band structure of them. So, the 4.5×10^5 sample was calculated, each corresponding to a unique configuration defined by the system size, impurity
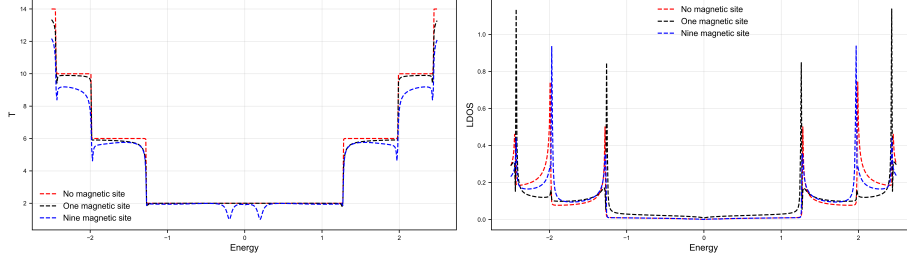
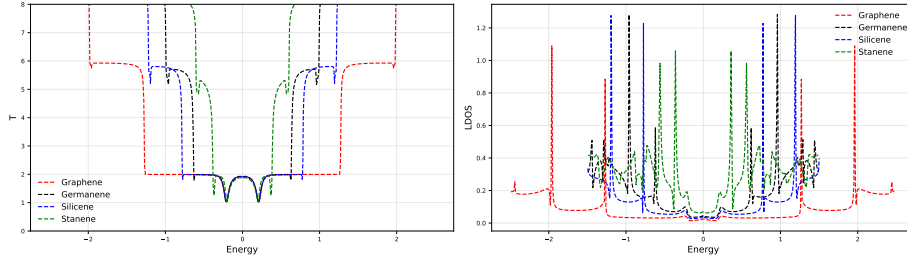Figure 2: $T(E)$ and $LDOS$ for three random magnetic configuration of graphene with w:16 and l=7

Figure 3: Comparison of T(E) and LDOS for materials with w=16, l=2, nm=3 used in the training dataset.

concentration, material type and energy. The dataset is divided into train and test, where test data are 20% of the whole.

The magnetic impurities, which were randomly distributed within the scattering region, introduce disorder into the system. The disorder generates complex quantum interference effects, making the transport quantities display very nonlinear behavior [33]. The nonlinearities are contained in the dataset and pose a challenging prediction task, as illustrated in (fig. 2). Also comparison of same configuration with equal number of magnetic impurity for graphene, germanene, silicene, and stanene; (fig. 3) show that T(E) and LDOS exhibit distinct behaviors. With an increase in the width of the system, there is a greater number of quantized steps in the transmission spectrum as a function of energy. This is the characteristic behavior of wider systems supporting more conducting channels. On the other hand, the introduction of magnetic impurities tends to smooth out these transmission steps by introducing scattering centers, which disrupt coherent transport. Additionally, impurities reduce the overall magnitude of both T(E) and LDOS near the Fermi energy, leading to the suppression of transport features. These results indicate the sensitivity of quantum transport properties to both disorder and geometrical parameters in the system. [34][21].

By considering our desired features, we have 8 inputs. Polynomial features used to capture nonlinear relationships between input features and target variables. Since transmission and LDOS in hexagonal lattices are affected by complex quantum interference and impurity scattering[35][36], their dependence on system parameters is often nonlinear. Transport properties are not simply proportional to lattice size or impurity concentration.

For each target, we train distinct models because of differences in values and their distributions. Since transmission and LDOS are continuous variables, a regression model is the natural choice. However,classification models require discrete labels. we discretized targets values by using $C = round[y]$, where C present classes. Convert continuous values into categories, making classification possible. To have fair comparison, grid space of valuse for searching best hyperparameters has been set equal for all models, and optimized parameters selected from them. To avoiding overfitting, k-fold method by setting k to 5 has been applied. Table 1 shows results of finetuning the models. We used scikit-

Model	n-estimators	max-depth	min-samples-split	PolynomialFeatures-degree
Model-1	100	50	2	3
Model-2	200	50	5	3
Model-3	200	20	2	2
Model-4	100	20	2	3

Table 1: Determined hyperparameters by grid search method for: Model-1: RF regression for T, Model-2: RF classifier for T, Model-3: RF regression for $LDOS$, Model-4: RF classifier for $LDOS$.

learn to train and evaluate performance [37]. (fig. 4) shows steps of our work. The hyperparameters tuned are the number of decision trees (n-estimators), the maximum depth of each tree (max-depth), the minimum number of samples required to split a node (min-samples-split), and the degree of polynomial features to include for input expansion. By selecting these parameters properly, we ensure that each model is properly fitted to capture the complex patterns in the data without overfitting. Interestingly, every model was enhanced by adding third-degree polynomial features, except for Model-3, where the optimal performance was achieved with a second-degree expansion, likely due to the fact that LDOS changes relatively more smoothly than transmission.

By training models on training data, performance of models has evaluate, table 2 shows performance for predict transmissions values as target and table 3 is for $LDOS$ as target. MAE, RMSE and R^2 typically used to measure performance of regression models. As we compare classification versus regression we should have same measure metric, So, for claculating accuracy as how many classes predictions were correct out of all predictions and F1 that computes the average of precision and recall, continues predicted values of regression were converted by rounding to classes. On the other hand, for compute regression metrics for classification task, we consider classes that produced by rounding as actual values of targets.

Table 2 shows that the regression model significantly outperforms the clas-
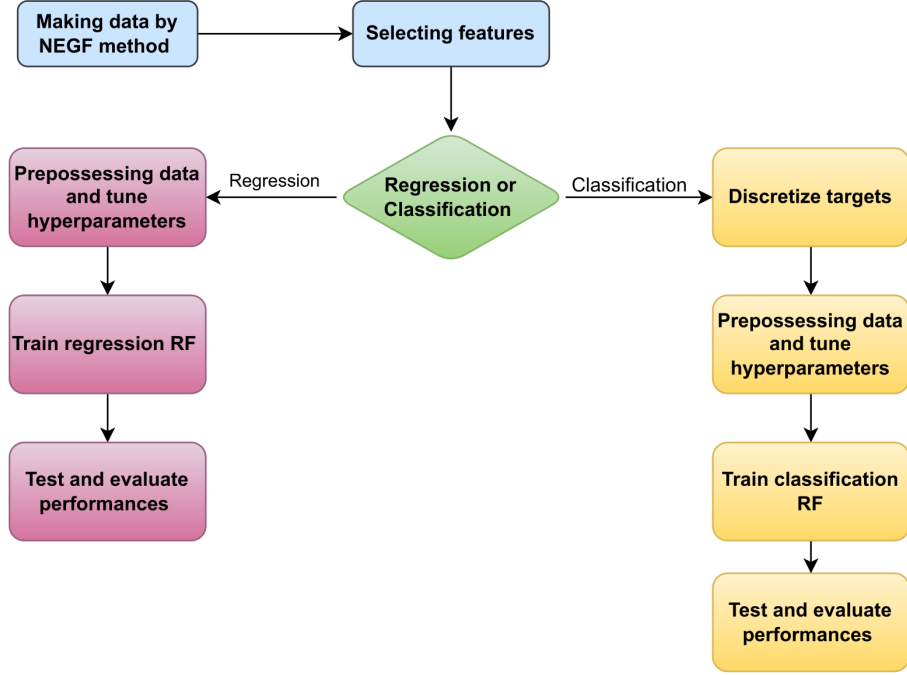
7

Figure 4: flowchart of how we train and evaluate models

Model	MAE	RMSE	R^2	Accuracy	F1
Model-1	0.0173	0.0620	0.9998	0.9834	0.9833
Model-2	0.0254	0.1656	0.9990	0.9751	0.9753

Table 2: Performance of models to predict T on test data

Model	MAE	RMSE	R^2	Accuracy	F1
Model-3	0.0085	0.0836	0.8474	0.9534	0.9535
Model-4	0.1002	1.1394	0.7266	0.9598	0.9591

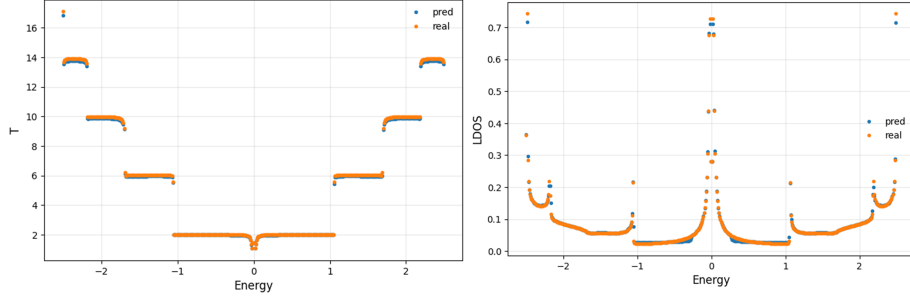Table 3: Performance of models to predict $LDOS$ on test data

Figure 5: predict T and LDOS values for random configuration from the test dataset

Target	MAE	RMSE	R^2	Accuracy	F1
$LDOS$	0.0390	0.0637	0.2899	0.7060	0.7153
T	0.5562	0.9563	0.9845	0.6240	0.7027

Table 4: Performance of models to predict T on extrapolation data

sification model for predicting T. The regression model achieves an MAE score of 0.0173, compared to the classification model's MAE of 0.0254; indicating more precise predictions. Also, the lower accuracy and F1-score for classification indicate that rounding leads to a loss of precision in capturing variations in T.

Similarly, Table 3 shows that regression is also superior for $LDOS$ predictions, with MAE=0.0085, whereas classification achieves an MAE of 0.1002. The classification model struggles with capturing finer variations in LDOS due to discretization effects. Discretizing continuous values by rounding leads to information loss and this approach affects on performance of RF classification. While classification models achieve high accuracy and F1-score, they suffer from information loss due to rounding. This explains why regression models consistently achieve higher scores. Classification forces continuous values into discrete bins, making it unable to capture small variations in T and $LDOS$ that regression can learn directly. (fig. 5) shows the results of using RF regression as a selected model in one of the random configurations in the test dataset. The results agree with the performance metrics.

To evaluate the models' performance on extrapolation data—system configurations outside the training range, we generated a test dataset in the systems shape of: $w : 36, L : 2, nm : 5$ and predict targets with our models. Table 4 presents the performance of our models on extrapolation data. Significant decrease in performances are observed: the accuracy of the RF regression model for T drops by 32%, and for $LDOS$, it drops by 25%. The overall degradation in performance across all metrics highlights a fundamental limitation of RF models. (fig. 6) is the predicted values versus reals of graphene sample where shows
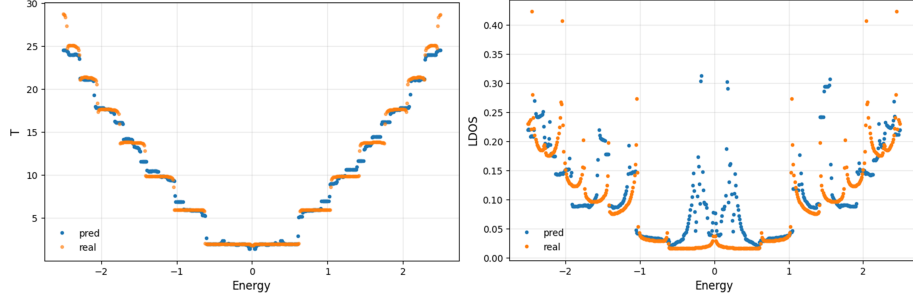
9

Figure 6: predict T and LDOS values for extrapolation data of graphene system

that the Random Forest model struggles with extrapolation. While it performs well on training and test data, its accuracy drops significantly when applied to configurations outside the training range. This is because RF builds decision trees based on thresholds observed during training, and when features exceed these thresholds, the model lacks meaningful rules to guide predictions. As a result, it often defaults to predictions from boundary regions of the training set, leading to poor generalization.

Random Forest (RF) has been successfully applied in previous works to classify T, demonstrating its ability to capture transport patterns[15] [38]. However, such models typically focus on small-scale systems or limited feature sets, and do not address scalability across material types and device geometries. In this work, we extend the analysis by testing RF in both regression and classification settings while ensuring the model can generalize to larger system sizes and impurity levels. Importantly, we assess the models' limitations by testing them on extrapolation data — a critical step often missing in similar works. These results clearly demonstrate both the practical value and boundaries of Random Forest models in quantum transport prediction.

4 conclusion

Here, we built data-driven and scalable machine learning models to predict key quantum transport quantities—namely, the transmission coefficient T(E) and the local density of states (LDOS)—in hexagonal two-dimensional (2D) lattices with randomly located magnetic impurities. The model for the physical system was a tight-binding Hamiltonian, and the transport quantities were computed using the Non-Equilibrium Green's Function (NEGF) formalism. By constructing a dataset that spans a broad range of device geometries, impurity concentrations, and energy levels, we ensured that our models learned from physically valid and diverse configurations. Features were selected based on the geometric and physical characteristics of the lattice; including the width and length of the scattering region, number of impurities, hopping amplitude, and target energy. Our results reveal that Random Forest regression models

are superior to classification-based approaches in accuracy, stability, and the ability to learn continuous variations in quantum transport behavior. Regression models possessed extremely low error measures and very high R^2 scores on test data, successfully learning the underlying nonlinear relationships created by impurity-induced disorder and interference effects.

However, although these models were excellent on in-domain data, they degraded severely when evaluated on extrapolation scenarios, i.e., device configurations outside the training interval. This finding is particularly crucial for researchers wishing to deploy these models in actual applications where configurations unheard of elsewhere dominate.

The predictive accuracy of our method offers significant advantage in the high-throughput screening and optimization of 2D material devices, particularly in spintronics and nanoelectronics, where computationally costly calculations are frequent. By replacing expensive quantum transport calculations with cheap and accurate machine learning models, researchers can accelerate the design process and better use computational resources.

In the future, one can look forward to seeing further work in the direction of merging more expressive and adaptive learning frameworks—such as Physics-informed neural networks (PINNs) , graph neural networks, or Gaussian processes—to improve generalization, especially in extrapolation regimes. Further, opening up the input feature space to include spin-orbit coupling, edge geometries, temperature effects, or even strain and external fields would help to further improve the physical accuracy and predictive power of the model. These developments would allow the models to be used for a broader class of materials and device geometries, ultimately pushing the limits of machine learning in quantum transport.

References

[1] Y.-C. Lin, R. Torsi, R. Younas, C. L. Hinkle, A. F. Rigosi, H. M. Hill, K. Zhang, S. Huang, C. E. Shuck, C. Chen, *et al.*, "Recent advances in 2d material theory, synthesis, properties, and applications," *ACS nano*, vol. 17, no. 11, pp. 9694–9747, 2023.

[2] P. Ares and K. S. Novoselov, "Recent advances in graphene and other 2D materials," *Nano Materials Science*, vol. 4, pp. 3–9, Mar. 2022.

[3] N. Mounet, M. Gibertini, P. Schwaller, D. Campi, A. Merkys, A. Marrazzo, T. Sohier, I. E. Castelli, A. Cepellotti, G. Pizzi, and N. Marzari, "Two-dimensional materials from high-throughput computational exfoliation of experimentally known compounds," *Nat. Nanotechnol.*, vol. 13, pp. 246–252, Mar. 2018.

[4] H. Ding, Z. Zhen, H. Imtiaz, W. Guo, H. Zhu, and B. Liu, "Why are most 2D lattices hexagonal? the stability of 2D lattices predicted by a simple mechanics model," *Extreme Mech. Lett.*, vol. 32, p. 100507, Oct. 2019.

[5] E. C. Ahn, "2D materials for spintronic devices," *Npj 2D Mater. Appl.*, vol. 4, June 2020.

[6] V. Sharma, P. Srivastava, and N. K. Jaiswal, "Prospects of asymmetrically h-terminated zigzag germanene nanoribbons for spintronic application," *Appl. Surf. Sci.*, vol. 396, pp. 1352–1359, Feb. 2017.

[7] G. B. Lesovik and I. A. Sadovskyy, "Scattering matrix approach to the description of quantum electron transport," *Physics-Uspekhi*, vol. 54, no. 10, p. 1007, 2011.

[8] I. Rungger, A. Droghetti, and M. Stamenova, "Non-equilibrium green's function methods for spin transport and dynamics," in *Handbook of Materials Modeling*, pp. 957–983, Cham: Springer International Publishing, 2020.

[9] S. Datta, *Quantum Transport*. Cambridge, England: Cambridge University Press, June 2012.

[10] J. Fang, M. Xie, X. He, J. Zhang, J. Hu, Y. Chen, Y. Yang, and Q. Jin, "Machine learning accelerates the materials discovery," *Mater. Today Commun.*, vol. 33, p. 104900, Dec. 2022.

[11] Y. Jing, H. Chu, B. Huang, J. Luo, W. Wang, and Y. Lai, "A deep neural network for general scattering matrix," *Nanophotonics*, vol. 12, pp. 2583–2591, June 2023.

[12] A. Lopez-Bezanilla and O. A. von Lilienfeld, "Modeling electronic quantum transport with machine learning," *Phys. Rev. B Condens. Matter Mater. Phys.*, vol. 89, June 2014.

[13] T. W. Ko, J. A. Finkler, S. Goedecker, and J. Behler, "A fourth-generation high-dimensional neural network potential with accurate electrostatics including non-local charge transfer," *Nat. Commun.*, vol. 12, p. 398, Jan. 2021.

[14] Y. Jia, X. Hou, Z. Wang, and X. Hu, "Machine learning boosts the design and discovery of nanomaterials," *ACS Sustain. Chem. Eng.*, vol. 9, pp. 6130–6147, May 2021.

[15] K. J. B. Ghosh and S. Ghosh, "Classical and quantum machine learning applications in spintronics," *Digit. Discov.*, vol. 2, no. 2, pp. 512–519, 2023.

[16] N. B. Le, T. D. Huan, and L. M. Woods, "Tunable spin-dependent properties of zigzag silicene nanoribbons," *Phys. Rev. Appl.*, vol. 1, June 2014.

[17] Y.-C. Zhao and J. Ni, "Spin-semiconducting properties in silicene nanoribbons," *Physical Chemistry Chemical Physics*, vol. 16, no. 29, pp. 15477–15482, 2014.

[18] J.-K. Lyu, S.-F. Zhang, C.-W. Zhang, and P.-J. Wang, "Stanene: A promising material for new electronic and spintronic applications," *Ann. Phys.*, vol. 531, p. 1900017, Oct. 2019.

[19] M. Ezawa, "Monolayer topological insulators: Silicene, germanene, and stanene," *J. Phys. Soc. Jpn.*, vol. 84, p. 121003, Dec. 2015.

[20] T. C. Li and S.-P. Lu, "Quantum conductance of graphene nanoribbons with edge defects," *Phys. Rev. B Condens. Matter Mater. Phys.*, vol. 77, Feb. 2008.

[21] N. Rahmani Ivriq, A. Ahmadkhan Kordbacheh, and M. Kargar Kheirabadi, "Quantum conductance of defected phosphorene and germanene nanoribbons," *J. Nanopart. Res.*, vol. 21, Nov. 2019.

[22] C.-C. Liu, H. Jiang, and Y. Yao, "Low-energy effective hamiltonian involving spin-orbit coupling in silicene and two-dimensional germanium and tin," *Phys. Rev. B Condens. Matter Mater. Phys.*, vol. 84, Nov. 2011.

[23] M. A. R. Faisal, Y. Wong, N. E. Alias, T. S. Tan, C. S. Lim, and M. L. P. Tan, "Electronic properties of stanene nanoribbon using tight binding method," *J. Nanotechnol.*, vol. 2025, Jan. 2025.

[24] L. Breiman *Mach. Learn.*, vol. 45, no. 1, pp. 5–32, 2001.

[25] L. Auret and C. Aldrich, "Interpretation of nonlinear relationships between process variables by use of random forests," *Miner. Eng.*, vol. 35, pp. 27–42, Aug. 2012.

[26] R. Genuer, J.-M. Poggi, C. Tuleau-Malot, and N. Villa-Vialaneix, "Random forests for big data," *Big Data Res.*, vol. 9, pp. 28–46, Sept. 2017.

[27] N. Amor, M. T. Noman, and M. Petru, "Prediction of functional properties of nano [formula: see text] coated cotton composites by artificial neural network," *Sci. Rep.*, vol. 11, p. 12235, June 2021.

[28] O. P. D, P. S. Babu, I. V, A. B, V. S, and K. C, "Enhanced SOC estimation of lithium ion batteries with RealTime data using machine learning algorithms," *Sci. Rep.*, vol. 14, p. 16036, July 2024.

[29] T. O. Owolabi and M. A. Abd Rahman, "Prediction of band gap energy of doped graphitic carbon nitride using genetic algorithm-based support vector regression and extreme learning machine," *Symmetry (Basel)*, vol. 13, p. 411, Mar. 2021.

[30] A. C. Rajan, A. Mishra, S. Satsangi, R. Vaish, H. Mizuseki, K.-R. Lee, and A. K. Singh, "Machine-learning-assisted accurate band gap predictions of functionalized MXene," *Chem. Mater.*, vol. 30, pp. 4031–4038, June 2018.

[31] Y. Zhang, W. Xu, G. Liu, Z. Zhang, J. Zhu, and M. Li, "Bandgap prediction of two-dimensional materials using machine learning," *PLoS One*, vol. 16, p. e0255637, Aug. 2021.

[32] K. Maertens, J. D. Baerdemaeker, and R. Babuška, "Genetic polynomial regression as input selection algorithm for non-linear identification," *Soft Comput.*, vol. 10, pp. 785–795, July 2006.

[33] A.-M. Visuri, T. Giamarchi, and C. Kollath, "Nonlinear transport in the presence of a local dissipation," *Phys. Rev. Res.*, vol. 5, Mar. 2023.

[34] A. A. Kordbacheh, A. Jafari, M. Ghoranneviss, and M. Hantehzadeh, "Effects of localized disorder on the quantum transport property of a four-terminal graphene nanodevice," *J. Comput. Theor. Nanosci.*, vol. 11, pp. 1779–1784, Aug. 2014.

[35] P. O. Sukhachov and A. V. Balatsky, "Non-Hermitian impurities in dirac systems," *Phys. Rev. Res.*, vol. 2, Mar. 2020.

[36] A. Kordbacheh, A. Jafari, and M. Arjmand, "Abnormal electronic transport in disordered four-terminal graphene nanodevice," *J. Theor. Appl. Phys.*, vol. 7, no. 1, p. 54, 2013.

[37] F. Pedregosa, G. Varoquaux, A. Gramfort, V. Michel, B. Thirion, O. Grisel, M. Blondel, P. Prettenhofer, R. Weiss, V. Dubourg, J. Vanderplas, A. Passos, D. Cournapeau, M. Brucher, M. Perrot, and E. Duchesnay, "Scikit-learn: Machine learning in Python," *Journal of Machine Learning Research*, vol. 12, pp. 2825–2830, 2011.

[38] T. Wu and J. Guo, "Speed up quantum transport device simulation on ferroelectric tunnel junction with machine learning methods," *IEEE Transactions on Electron Devices*, vol. 67, no. 11, pp. 5229–5235, 2020.